Aminolysis of Dicationic Ruthenium Thiophene Complexes

Qian Feng, Thomas B. Rauchfuss,* and Scott R. Wilson

School of Chemical Sciences, University of Illinois, Urbana, Illinois 61801

Received February 8, 1995[⊗]

Dicationic sandwich complexes containing thiophene, 2-methylthiophene, 2,5-dimethylthiophene, and tetramethylthiophene react with ammonia to give salts of the formula [(ring)-$Ru(SC_4R_4NH_2)$]X where ring = C_6Me_6 or cymene. The thiophene, 2-methylthiophene, and 2,5-dimethylthiophene complexes undergo C–S cleavage to give iminium–thiolato derivatives. In the case of the 2,5-dimethylthiophene complex, a kinetic isomer was isolated which slowly isomerized to a thermodynamic isomer. The ammonia adducts of the tetramethylthiophene complexes $[(cymene)Ru(C_4Me_4S)]^{2+}$ and $[(C_5Me_5)Rh(C_4Me_4S)]^{2+}$ do not undergo C–S cleavage. These $2\text{-}NH_2C_4Me_4S$ complexes react with protic acids to regenerate the starting dication $[(ring)M(C_4Me_4S)]^{2+}$. The aniline adducts of thiophene, 2-methylthiophene, and 2,5-dimethylthiophene are similar to the ammonia derivatives. The structures of the kinetic isomer of $[(C_6Me_6)Ru(SC_3H_2MeCHNHPh)]PF_6$ and the thermodynamic isomer of $[(cymene)Ru(SC_3H_2MeCMeNHPh)]OTf$ were established by single-crystal X-ray diffraction. The crystallographic study proves that the isomerization in this family of compounds arises from the relative configuration at the terminal carbon of the alkenyl thiolate ligand. Bond distance data indicate an interaction between the iminium carbon center and the Ru atom in the kinetic isomer.

Introduction

In previous papers we have described the reactions of dicationic thiophene complexes with hydroxide.[1–3] The work was motivated by the prospect of developing nonconventional methods for the desulfurization of thiophenes.[4] The chemistry proved to be particularly rich, leading to the isolation of four isomeric forms of oxygenated thiophene ligands C_4Me_4SO (Chart 1). This work provided the first evidence for nucleophilic addition to the sulfur center of thiophene. In addition, the hydrolyzed thiophene complexes display extensive ligand-based reactions.[2] Variants of the base hydrolysis reaction of coordinated thiophenes are of interest in that they illustrate new pathways for breaking C–S bonds.

Nucleophilic addition to metal arene complexes has been recognized for many years.[5,6] The first extension of this pattern to thiophene complexes was provided by studies on nucleophilic addition to thiophene complexes of $Mn(CO)_3^+$ and $(C_5H_5)Ru^+$.[7,8] For the Ru complexes, these reactions result in C–S bond cleavage and show some potential for the synthesis of organo–sulfur

Chart 1

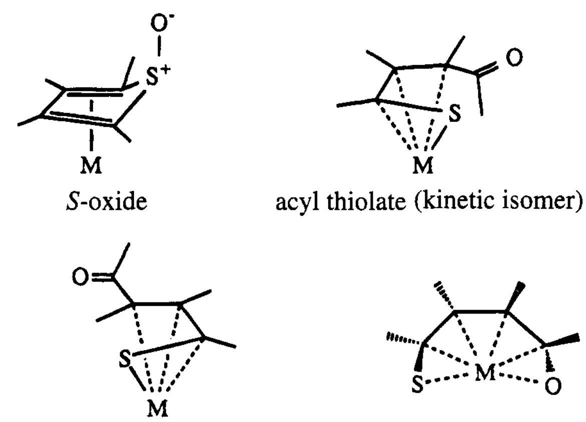

S-oxide; acyl thiolate (kinetic isomer); acyl thiolate (thermodynamic isomer); η^6-acyl thiolate

compounds. Our recent studies[2,3] on base hydrolysis focused on dicationic arene–thiophene complexes (ring)-$Ru(C_4R_4S)^{2+}$ (ring = C_4Me_4S, cymene, and hexamethylbenzene) and $(C_5Me_5)Rh(C_4Me_4S)^{2+}$. The (arene)$Ru^{2+}$ moiety is of particular interest since it forms stable adducts of most thiophenes[9,10] and the resulting dicationic sandwich complexes are highly electrophilic. The present work deals with their reactions with ammonia and aniline. These results provide new methods of C–S cleavage with common reagents. The associated structural studies clarify the mechanistic and stereochemical facets of nucleophilic addition to η^5-thiophene ligands.

⊗ Abstract published in *Advance ACS Abstracts,* May 15, 1995.

(1) Skaugset, A. E.; Rauchfuss, T. B.; Wilson, S. R. *J. Am. Chem. Soc.* **1992**, *114*, 8521.
(2) Krautscheid, H.; Feng, Q.; Rauchfuss, T. B. *Organometallics* **1993**, *12*, 3273.
(3) Feng, Q.; Krautscheid, H.; Rauchfuss, T. B.; Skaugset, A. E.; Venturelli, A. *Organometallics* **1995**, *14*, 297.
(4) (a) Ogilvy, A. E.; Draganjac, M. E.; Rauchfuss, T. B.; Wilson, S. R. *Organometallics* **1988**, *7*, 1171. (b) Riaz, U.; Curnow, O.; Curtis, D. M. *J. Am. Chem. Soc.* **1991**, *113*, 1416. (c) Garcia, J. J.; Mann, B. E.; Adams, H.; Bailey, N. A.; Maitlis, P. M. *J. Am. Chem. Soc.* **1995**, *117*, 2179.
(5) Hegedus, L. S. *Transition Metals in the Synthesis of Complex Organic Molecules*; University Science Books: Mill Valley, CA, 1994.
(6) Kane-Maguire, L. A. P.; Honig, E. D.; Sweigart, D. A. *Chem. Rev.* **1984**, *84*, 525.
(7) Lesch, D. A.; Richardson, J. W.; Jacobson, R. A.; Angelici, R. J. *J. Am. Chem. Soc.* **1984**, *106*, 2901.
(8) Hachgenei, J. W.; Angelici, R. J. *J. Organomet. Chem.* **1988**, *355*, 359. Spies, G. H.; Angelici, R. J. *Organometallics* **1987**, *6*, 1897.
(9) Ganja, E. A.; Rauchfuss, T. B.; Stern, C. L. *Organometallics* **1991**, *10*, 270.
(10) Luo, S.; Rauchfuss, T. B.; Wilson, S. R. *J. Am. Chem. Soc.* **1992**, *114*, 8515.
(11) Dalmay, L.-V.; Colthup, N. B.; Fateley, W. G.; Grasselli, J. G. *The Handbook of Infrared and Raman Characteristic Frequencies of Organic Molecules*; Academic Press: New York, 1991; p 200.

Results

Ammonolysis of C_4H_4S and $2\text{-}MeC_4H_3S$ Complexes. We started with the addition of the simplest amine, ammonia, to a complex of the simplest thiophene, $[(C_6Me_6)Ru(C_4H_4S)](OTf)_2$. Treatment of the solid ruthenium complex with gaseous ammonia resulted in a rapid color change from yellow to red. The product was purified by simple extraction into CH_2Cl_2 and filtration from the NH_4OTf. This new compound analyzed as $[(C_6Me_6)Ru(SC_3H_3CHNH_2)]OTf$ (**1**, eq 1; in this and subsequent equations, the spectator η^6-arene ligand is not shown).

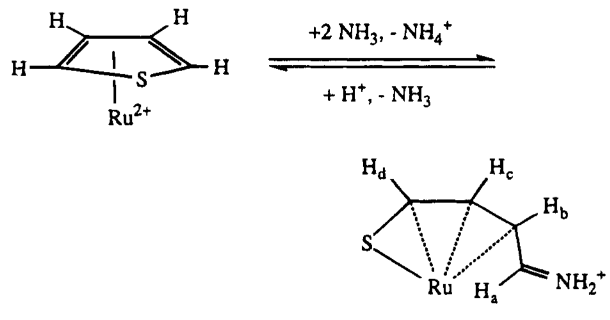

(1)

1

The IR spectrum of **1** shows a moderately strong band at 1620 cm^{-1} assigned to $\nu_{C=N}$ and strong bands at 3336 and 3208 cm^{-1} assigned to ν_{NH}. The ^{1}H NMR spectrum was analyzed by decoupling and difference nOe experiments that probed the relative positions of the $SC_4H_4NH_2$ protons. Three of the thiophene-derived signals showed strong nOe's, indicating that they are cis and coplanar. For instance, irradiation of H_b increases the intensity H_c, which is cis, by 15%, and at the same time only a much smaller (3%) nOe is observed for the trans H_a. This solution structure is consistent with the results of a single-crystal structural analysis of an analogous complex (*vide infra*). Solutions of **1** revert to the starting complex $[(C_6Me_6)Ru(C_4H_4S)]^{2+}$ upon treatment with triflic acid.

Ammonolysis of the 2-methylthiophene complex afforded a related product, $[(cymene)Ru(SC_3H_2MeCHNH_2)]OTf$ (**2**) (eq 2). The addition and C–S cleavage processes

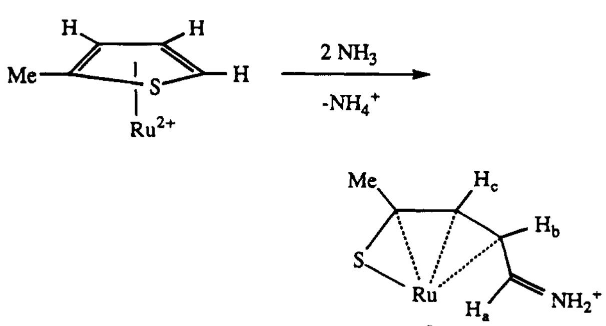

(2)

2

occur regiospecifically at the CH–S linkage, not at C(Me)–S. The presence of only one isomer was established by ^{1}H NMR spectroscopy, which, for instance, showed only one set of cymene resonances. The $CH{=}NH_2^+$ signal was found in a position similar to that for the aforementioned thiophene product. Angelici had previously observed that nucleophiles (OR^-, H^-, CR_3^-) selectively add to the unsubstituted carbon in $(C_5H_5)Ru(2\text{-}MeC_4H_3S)^+$.[8]

Ammonolysis of $[(cymene)Ru(2,5\text{-}Me_2C_4H_2S)]^{2+}$. Additional stereochemical insights into the ammonolysis reaction were provided by studies on the dimethylthiophene complex $[(cymene)Ru(2,5\text{-}Me_2C_4H_2S)]^{2+}$. Acetonitrile solutions of this salt reacted readily with ammonia. When the reaction was allowed to proceed for a brief interval, we obtained pure samples of a single isomer of $[(cymene)Ru(SC_3H_2MeCMeNH_2)]^+$ (**3**$_{\mathbf{kin}}$). The spectroscopic evidence supports a structure analogous to those of the aforementioned products derived from thiophene and 2-methylthiophene complexes. The ^{1}H and ^{13}C NMR data point to a chiral complex, and the IR spectrum shows bands attributable to both ν_{NH} (3346 and 3153 cm^{-1}) and $\nu_{C=N}$ (1648 cm^{-1}).[11] Care must be taken in this synthesis because the product tends to isomerize (see below). The degree of isomerization can be minimized by conducting the ammonolysis on solid samples of $[(cymene)Ru(2,5\text{-}Me_2C_4H_2S)](OTf)_2$.

In solution, **3** isomerizes via a first-order process with $t_{1/2}$ = 54 min (35 °C). Notice that, according to this mechanism, isomerization does not result in racemization. We refer to these isomers as kinetic and thermodynamic, **3**$_{\mathbf{kin}}$ and **3**$_{\mathbf{therm}}$, respectively (eq 3). It was

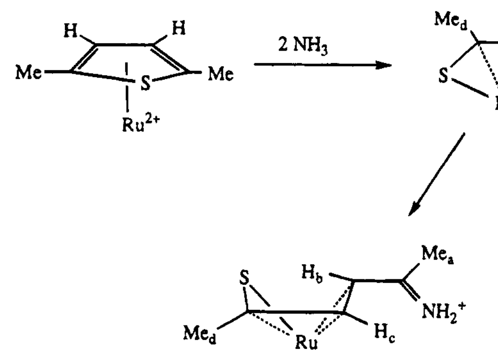

(3)

3$_{\mathbf{kin}}$ **3**$_{\mathbf{therm}}$

found that solid samples of **3**$_{\mathbf{kin}}$ rearranged upon standing at 30 °C.

The spectroscopic characteristics of the **3**$_{\mathbf{kin}}$ and **3**$_{\mathbf{therm}}$ isomers are similar. The UV–vis spectra differ only slightly even though the isomers have noticeably different colors, the kinetic isomer being more red while the other isomer is more purple. The $C_4H_2Me_2$ signals on the thiophene are most sensitive to the identity of the isomer. The ^{1}H NMR shift for H_b occurs at 3.88 ppm for **3**$_{\mathbf{kin}}$ and 1.80 ppm for **3**$_{\mathbf{therm}}$. Attempts to isomerize **1** and **2** led only to unidentified decomposition products.

Solutions of **3**$_{\mathbf{kin}}$ were shown to react with aqueous KOH to give the kinetic isomer of the corresponding acyl thiolate[2] (eq 4).

Ammonolysis of C_4Me_4S Complexes. To our initial surprise, the ammonolysis of tetramethylthiophene complexes proceeds rather differently from the cases for less substituted thiophenes. Solutions of the tetramethylthiophene complexes $[(cymene)Ru(C_4Me_4S)]^{2+}$ and $[(C_5Me_5)Rh(C_4Me_4S)]^{2+}$ react with ammonia to give orange-yellow microcrystalline adducts $[(ring)M(C_4Me_4S\text{-}2\text{-}NH_2)]^+$ (M = Ru, ring = cymeme (**4**); M = Rh, ring = C_5Me_5 (**5**)). The ^{1}H NMR data for **4** indicate that it is

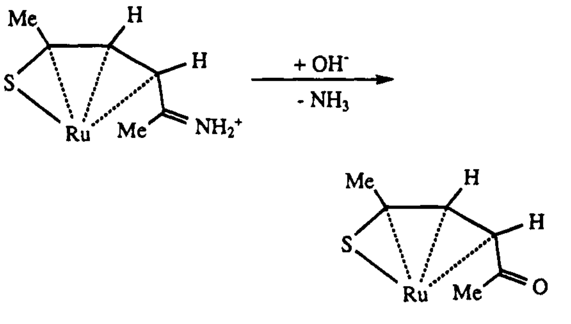

(4)

chiral as we observe four $MeC_6H_4CHMe_2$ multiplets. Its IR spectrum is dominated by a strong band at 3300 cm^{-1} corresponding to ν_{NH}. We do not observe strong bands in the range for $\nu_{C=N}$, as seen in the amine derivatives of other thiophenes. Solutions of **4** react with HOTf to recover the starting $[(cymene)Ru(C_4Me_4S)]^{2+}$.

The ^{1}H NMR data for **5** proved comparable to those for **4**, with the exception of a signal for one methyl group which is split due to ^{103}Rh coupling. This long-range splitting had been previously observed for $[(C_5Me_5)Rh(C_4Me_4S\text{-}2\text{-}OH)]^+$, which was shown by crystallography to feature an η^4-C_4Me_4S-2-OH ligand.[1] Solutions of **5** react with HOTs to regenerate the starting $[(C_5Me_5)Rh(C_4Me_4S)]^{2+}$ (eq 5).

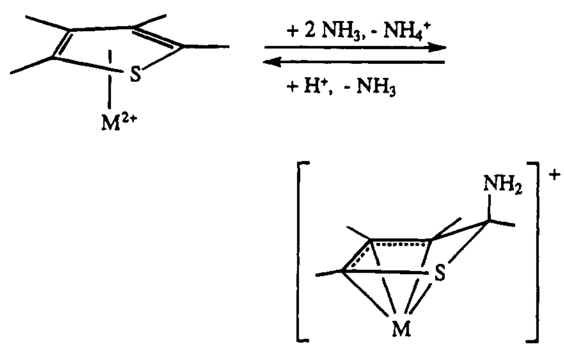

(5)

M = Ru(cymene) (4), Rh(C_5Me_5) (5)

Reactions with Aniline. The corresponding reactions of the dicationic thiophene complexes with aniline were also examined in an attempt to probe the generality of the amination. These experiments also afforded X-ray-quality crystals of both kinetic and thermodynamic isomers. The complexes of thiophene and 2-methylthiophene $[(C_6Me_6)Ru(C_4H_{4-x}Me_xS)]^{2+}$ (x = 0, 1) reacted readily with aniline to give deep red crystalline products $[(C_6Me_6)Ru(SC_3H_3CHNHPh)]OTf$ (**6**) and $[(C_6Me_6)Ru(SC_3H_2MeCHNHPh)]PF_6$ (**7**), respectively (eq 6).

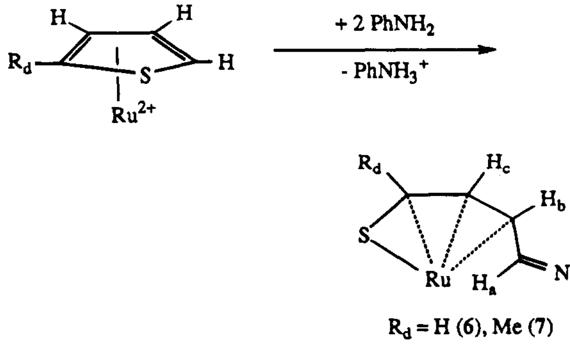

(6)

R_d = H (6), Me (7)

In both cases, the ^{1}H NMR spectra indicated single isomers whose spectroscopic properties were consistent with the aforementioned kinetic isomers. The critical data were the chemical shift and coupling patterns for the protons on the thiolate ligand.

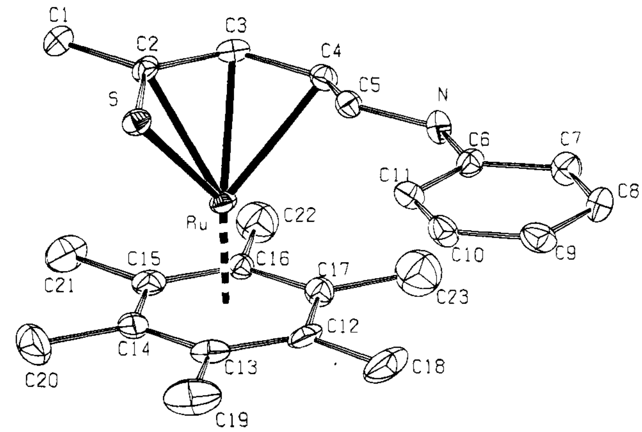

Figure 1. ORTEP plot of one of two enantiomeric cations in the salt $[(C_6Me_6)Ru(\eta^4\text{-}SC_3H_2MeCHNHPh)]PF_6$ (**7**).

The addition of aniline to $[(cymene)Ru(2,5\text{-}Me_2C_4H_2S)]^{2+}$ was also rapid; however, in this case we only obtained the thermodynamic isomer of $[(cymene)Ru(SC_3H_2MeCMeNHPh)]OTf$ ($\mathbf{8_{therm}}$). Actually, the ^{1}H NMR data revealed what appear to be two thermodynamic isomers in a ratio of 4:1. Since the chemical shift and coupling patterns for the two are quite similar, we suggest that these species differ according to the relative orientation of the phenyl substituent on the iminium nitrogen center. The rapid formation of the thermodynamic isomer(s) suggests that the presence of the phenyl group destabilizes $\mathbf{8_{kin}}$. The elusive $\mathbf{8_{kin}}$ was observed when the reaction was monitored by ^{1}H NMR spectroscopy at −10 °C.

Using $\mathbf{8_{therm}}$, we demonstrated amine exchange, in that treatment of a solution of this salt with an excess of ammonia gave free aniline and the aforementioned $\mathbf{3_{therm}}$, as demonstrated by ^{1}H NMR studies (eq 7).

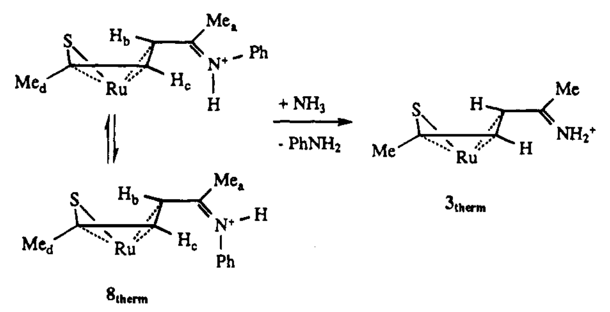

(7)

Crystallographic Studies on $[(C_6Me_6)Ru(SC_3H_2MeCHNHPh)]PF_6$ (7) and $[(cymene)Ru(SC_3H_2MeCMeNHPh)]OTf$ ($\mathbf{8_{therm}}$). The spectroscopic evidence that $\mathbf{8_{therm}}$ is stable only as the thermodynamic isomer was confirmed by the crystallographic analysis. The connectivity and metrical details are unexceptional. The assignment of this species as an iminium derivative is supported by the bond distances and angles at C5; the C=N distance of 1.34(2) Å is appropriate for a double bond and far shorter than the bond between nitrogen and phenyl (1.47(2) Å) (Figure 2).

The structure of **7** in the solid state reveals a sandwich structure wherein the thiophene ligand is cleaved (Figure 1). The bond distances and angles in the C_3S portion of the ligand are similar to those found

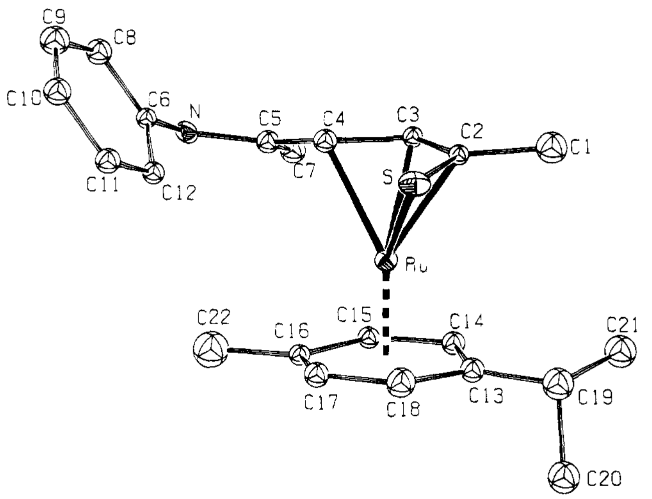

Figure 2. ORTEP plot of one of two enantiomeric cations in the salt [(cymene)Ru(η^4-SC_3H_2MeCMeNHPh)]OTf ($\mathbf{8_{therm}}$).

in $\mathbf{8_{therm}}$. It is seen that the nucleophile has added to the less substituted carbon α to sulfur. Furthermore, the stereochemistry of the carbon γ to sulfur is consistent with the kinetic isomer, as assigned in previous papers dealing with acyl analogues.[2] This compound is not a direct analogue of an acyl, since it is an iminium derivative, not an imine. Related to this difference is some ambiguity in classifying the iminium thiolate as an η^4 ligand. The iminium carbon C5 is situated 2.627 Å from Ru, vs 2.192(5), 2.222(10), and 2.288(6) Å for Ru−C2, −C3, and −C4, respectively. For comparison, the iminium C−Ru distance is 3.08 Å in $\mathbf{8_{therm}}$.

Discussion

Dicationic π-thiophene complexes readily add ammonia and amines.[12] The transformations are efficient, and the scope of the reaction appears to be broad. The structural chemistry is consistent with, but more complete than, other cases of nucleophilic additions to dicationic thiophene complexes. The results are especially relevant to our studies on the base hydrolysis of thiophene complexes.[2] Meriting further discussion are mechanistic relationships and structural trends in these compounds.

The structural chemistry of these compounds is controlled by a number of subtle but systematic factors even though all of the ammonia derivatives have the same basic formula (arene)Ru($C_4R_4SNH_2$)$^+$. The amination of tetramethylthiophene complexes afforded ring-closed structures, analogous to that of (C_5Me_5)Rh(C_4Me_4S-2-OH)$^+$.[1] The related dimethylthiophene complex on the other hand gives ring-opened isomers. We previously observed that ring opening depends on the degree of ring methylation for the species (C_6Me_6)Ru(C_4R_4HS)$^+$.[13]

For the first time, we have crystallographically confirmed the stereochemistry of a kinetic isomer of a ring-opened thiophene complex. One interesting detail of this structure is the Ru−iminium carbon distance of 2.627 Å, which is only 0.3 Å longer than other Ru−C distances in this complex. We also observe the isomerization of (cymene)Ru(SC_3H_2MeCMeNH_2)$^+$ whereby the kinetically formed endo isomer converts to the thermodynamically favored exo isomer, i.e., $\mathbf{3_{kin}}$ to $\mathbf{3_{therm}}$. The facility of the isomerization depends on the steric bulk of the added nucleophile as well as the substituents on thiophene.

Scheme 1

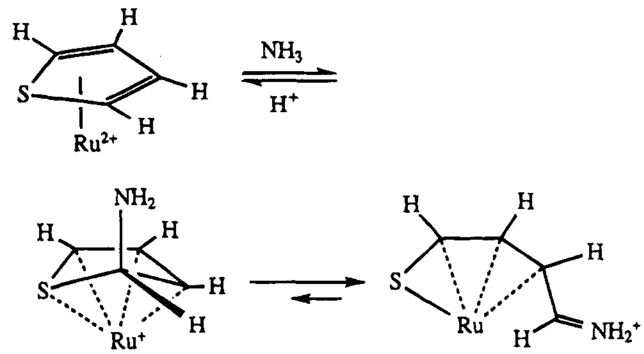

The products of the C−S cleavage reaction feature iminium centers. This assignment is supported by a number of factors including the details of the ^{1}H NMR spectra. The presence of two thermodynamic isomers for the $PhNH_2$ addition compound with 2,5-dimethylthiophene is also consistent with slow cis−trans isomerization at the iminium center. The crystallographic studies indicate that these iminium centers are conjugated via a π-bonding network with the rest of the allyl thiolate. The iminium carbon is demonstrably electrophilic, since it is susceptible to attack by OH^- (base hydrolysis) and NH_3 (transamination). This same reactivity pattern provides a plausible pathway for reclosure of the thiophene ring via nucleophilic attack of the thiolate on the imine carbon (Scheme 1). Recyclization of the thiophene ligand proceeds rapidly when the kinetic isomers are treated with protic sources. It was also found that the aminated ring-closed compounds derived from tetramethylthiophene revert to the dicationic sandwich structures upon treatment with acids.

The transformations reported in this paper are so well behaved that it is tempting to consider further extensions of these results. One possibility would be to attempt the reductive cleavage of the aminated thiophenes as a route to amino thiols.

Experimental Section

Materials and Methods. Hydrated ruthenium trichloride was obtained from PGM Ltd. (Gerrniston, Republic of South Africa), 2,5-dimethylthiophene from Penta, and AgOTf from Aldrich. Tetramethylthiophene and [(p-cymene)$RuCl_2$]$_2$ were prepared according to published procedures.[14] Syntheses and workups were performed under an inert atmosphere using purified nitrogen. The thiophene complexes have been described in previous publications.[1−3] The reagent grade solvents were distilled from Na/benzophenone (ether, THF, toluene, hexanes) or CaH_2 (acetonitrile, methylene chloride).

IR spectra were acquired on KBr pellets using a Mattson Galaxy Series FTIR 3000 spectrometer. NMR spectra were collected on a U-400 Varian spectrometer. Coupling patterns are described with the following abbreviations: s, singlet; d, doublet; t, triplet; dd doublet of doublets; ps, pseudo, br, broad. Coupling constants in hertz are indicated parenthetically. Field desorption mass spectra were measured on a VG 70-VSE

(12) In separate work we have demonstrated that alkylamines work well also: Kocazja, K. M.; Rauchfuss, T. B. Unpublished results.

(13) Luo, S.; Rauchfuss, T. B.; Gan, Z. *J. Am. Chem. Soc.* **1993**, *115*, 4943.

(14) Bennett, M. A.; Huang, T.-N.; Matheson, T. W.; Smith, A. K. *Inorg. Syntheses* **1982**, *21*, 74.

or a Finnigan MAT-731; fast atom bombardment spectra, on a VG ZAB-SE. Mass spectral data are reported in units of *m/z*. Elemental analyses were performed by the University of Illinois Microanalytical Laboratory.

[(C_6Me_6)Ru(η^4-$SC_3H_3CHNH_2$)]OTf (1). Anhydrous NH_3 was passed through a powdered sample of 300 mg (0.465 mmol) of [(C_6Me_6)Ru(C_4H_4S)]$(OTf)_2$ with stirring for 30 s. The resulting red solid was extracted into 10 mL of CH_2Cl_2. The extract was concentrated and diluted with 20 mL of hexanes giving a red powder. Yield: 203 mg (85%). ^1H NMR (CD_3-CN) (see eq 1 for labeling scheme): 7.02 (virtual q, J_{NH-H} = 11.0, $J_{4,3}$ = 11.5, 1H, H_a of $SC_3H_3CHNH_2$), 6.08 (dd, $J_{1,2}$ = 4.88, 1H, H_d of $SC_3H_3CHNH_2$), 6.02 (br s, 2H, NH_2), 5.58 (dd, $J_{2,3}$ = 6.6, 1H, H_c of $SC_3H_3HNH_2$), 3.99 (ddd, 1H, H_b of SC_3H_3-$CHNH_2$), 2.17 (s, 15H, C_6Me_6). $^{13}C\{^1H\}$ NMR (CD_3CN): 142.1 (C_a of $SC_3H_3CHNH_2$), 121.0 (q, CF_3), 100.8 (C_d of SC_3H_3-$CHNH_2$), 99.8 (C_6Me_6), 89.6 (C_c of $SC_3H_3CHNH_2$), 68.4 (C_b of $SC_3H_3CHNH_2$), 16.2 (C_6Me_6). IR (KBr): ν_{NH} = 3336 and 3208, $\nu_{C=N}$ = 1649 cm^{-1}. UV–vis: 500, 340 nm. FAB-MS: 364 (M^+). Anal. Calcd for $C_{17}H_{24}NF_3O_3RuS_2$: C, 39.83; H, 4.72; N, 2.73; Ru, 19.68; S, 12.51. Found: C, 39.97; H, 4.79; N, 2.80; Ru, 19.60; S, 12.36.

[(cymene)Ru(η^4-$SC_3H_2MeCHNH_2$)]OTf (2). Anhydrous NH_3 was passed over 200 mg (0.32 mmol) of solid [(cymene)-Ru(2-MeC_4H_3S)]$(OTf)_2$ for 30 s. The red oily product was extracted into 10 mL of CH_2Cl_2, and this extract was evaporated, leaving a red oil. Yield: 127 mg (80%). ^1H NMR (acetone-d_6) (see eq 2 for labeling scheme): 7.96 (br s, 2H, NH_2), 7.61 (br d, $J_{1,2}$ = 11.2 , 1H, H_a of $SC_3H_2MeCHNH_2$), 6.06 (d, 1H, $^iPrC_6H_4Me$), 5.94 (m, 2H, $^iPrC_6H_4Me$ and 1H, H_c of $SC_3H_2MeCHNH_2$), 5.60 (d, 1H, $^iPrC_6H_4Me$) , 4.52 (dd, $J_{2,1}$ = 11.2, $J_{2,3}$ = 6.4, 1H, H_b of $SC_3H_2MeCHNH_2$), 2.76 (sept, 1H, $CH(Me)_2C_6H_4Me$), 2.38 (s, 3H), 2.20 (s, 3H), 1.30 (dd, 6H, CH-$(Me)_2C_6H_4Me$). $^{13}C\{^1H\}$ NMR (CD_3CN): 158.5 (C_a of SC_3H_2-$MeCHNH_2$), 121.0 (q, CF_3), 113.7, 111.3 (C_d of SC_3H_2-$MeCHNH_2$), 100.2, 86.4, 85.9 (C_c of $SC_3H_2MeCHNH_2$), 85.8, 85.5, 84.3, 58.9 (C_b of $SC_3H_2MeCHNH_2$), 30.5, 28.3, 22.5, 21.8, 16.2. IR: ν_{NH} = 3328 and 3219, $\nu_{C=N}$ = 1651 cm^{-1}. UV–vis: 512 nm. FAB-MS: 350 (M^+). Anal. Calcd for $C_{16}H_{22}NF_3$-O_3RuS_2·$0.25CH_2Cl_2$: C, 37.56; H, 4.36; N, 2.69. Found: C, 37.87; H, 4.33; N, 2.51.

[(cymene)Ru(η^4-$SC_3H_2MeCMeNH_2$)]OTf (3_{kin}). Method a. Gaseous NH_3 was bubbled through a solution of 400 mg (0.62 mmol) of [(cymene)Ru(2,5-$Me_2C_4H_2S$)]$(OTf)_2$ in 20 mL of CH_3CN for 30 s. After a few minutes of stirring, the solvent was removed under vacuum. The red residue was extracted into 15 mL of CH_2Cl_2, leaving a white residue. The solution was filtered, and the filtrate was concentrated to 2 mL, followed by dilution with 20 mL of hexanes to give a red precipitate. Yield: 280 mg (89%).

Method b. Gaseous NH_3 was bubbled through 200 mg (0.31 mmol) of solid [(cymene)Ru($C_4H_2Me_2S$)]$(OTf)_2$ for 30 s. The red product was extracted into 10 mL of CH_2Cl_2. This extract was concentrated and diluted with 20 mL of hexanes resulting in a red precipitate. Yield: 142 mg (90%). ^1H NMR (CD_3CN) (see eq 3 for labeling scheme) 7.18 (br s, 2H, NH_2), 5.95 (ps d, 1H, $^iPrC_6H_4Me$), 5.68 (m, 2H, $^iPrC_6H_4Me$), 5.58 (ps d, 1H, $^iPrC_6H_4Me$), 5.40 (d, J = 5.4, 1H, H_c of SC_3H_2-$MeCMeNH_2$), 3.88 (d, J = 5.6, 1H, H_b of $SC_3H_2MeCMeNH_2$), 2.69 (sept, 1H, $CH(Me)_2C_6H_4Me$), 2.28 (s, 3H), 2.17 (s, 3H), 2.11 (s, 3H), 1.24 (dd, 6H, $CH(Me)_2C_6H_4Me$). $^{13}C\{^1H\}$ NMR (acetone-d_6): 175.2 (C_a of $SC_3H_2MeCMeNH_2$), 121.0 (q, CF_3), 111.3, 109.1 (C_d of $SC_3H_2MeCMeNH_2$), 98.3, 85.4, 84.7, 83.9, 83.8, 83.0 (C_c of $SC_3H_2MeCMeNH_2$), 49.5 (C_b of SC_3H_2-$MeCMeNH_2$), 31.6 ($CH(Me)_2C_6H_4Me$), 25.9, 22.8, 22.2, 22.1, 18.35. IR: ν_{NH} = 3381 and 3151, $\nu_{C=N}$ = 1648 cm^{-1}. UV–vis: 516, 388 nm. FAB-MS: 364 (M^+). Anal. Calcd for $C_{17}H_{24}$-$NF_3O_3RuS_2$: C, 39.83; H, 4.70; N, 2.73; Ru, 19.68; S, 12.50. Found: C, 39.60; H, 4.76; N, 2.73; Ru, 19.55; S, 12.46.

[(cymene)Ru(η^4-$SC_3H_2MeCMeNH_2$)]OTf (3_{therm}). A solid sample of the kinetic isomer was maintained at 45 °C. Over the course of 24 h, the red powder assumed a dark purple-red coloration. On the basis of ^1H NMR analysis, the transformation was quantitative. A solution of the kinetic isomer in CH_3-CN gave the thermodynamic isomer of [(cymene)Ru(η^4-SC_3H_2-$MeCMeNH_2$)]OTf after 12 h (~25 °C), which was isolated as a dark red oil. The kinetics of the isomerization were examined on 10 mg sample dissolved in 0.6 mL of CD_3CN, the solution of which was sealed in a 5 mm NMR tube. The progress of the reaction was monitored at 35 °C, and integrated spectra were recorded after 6 min, followed by 20 min intervals. Eight data points were collected. Plots of ln [3_{kin}] vs time were linear with a slope of $k = 2.13 \times 10^{-4}$ s^{-1}. ^1H NMR (acetone-d_6) (see eq 3 for labeling scheme): 9.93 (br s, 1H, NH_2), 9.68 (br s, 1H, NH_2), 6.17 (br d, 1H, H_c of $SC_3H_2MeCMeNH_2$), 6.07 (ps d, 1H, $^iPrC_6H_4Me$), 5.74 (ps d, 1H, $^iPrC_6H_4Me$), 5.59 (ps d, 1H, $^iPrC_6H_4Me$), 5.06 (ps d, 1H, $^iPrC_6H_4Me$), 2.72 (sept, 1H, $CH(Me)_2C_6H_4Me$), 2.40 (s, 3H, Me_a of $SC_3H_2MeCMeNH_2$), 2.38 (s, 3H, Me_d of $SC_3H_2MeCMeNH_2$), 2.16 (s, 3H, $CH(Me)_2C_6H_4Me$), 1.86 (br s, 1H, H_b of $SC_3H_2MeCMeNH_2$), 1.32 (dd, 6H, $CH(Me)_2C_6H_4Me$). $^{13}C\{^1H\}$ NMR (acetone-d_6): 191.7 (C_a of $SC_3H_2MeCMeNH_2$), 122.0 (q, CF_3), 110.5, 108.4 (C_d of SC_3H_2-$MeCMeNH_2$), 99.3, 86.7, 84.7, 84.6, 84.1 82.0 (C_c of SC_3H_2-$MeCMeNH_2$), 54.2 (C_b of $SC_3H_2MeCMeNH_2$), 31.7, 26.93, 26.90, 23.7, 23.4, 18.0. IR: ν_{NH} = 3328 and 3153, $\nu_{C=N}$ = 1668 cm^{-1}. UV–vis: 536, 418 nm. FAB-MS: 364 (M^+). Anal. Calcd for $C_{17}H_{24}NF_3O_3RuS_2$: C, 39.83; H, 4.70; N, 2.73; Ru, 19.68; S, 12.50. Found: C, 39.63; H, 4.66; N, 2.63; Ru, 19.38; S, 12.35.

Reaction of 3_{kin} with KOH. A solution of 30 mg (58.5 μmol) of [(cymene)Ru(η^4-$SC_3H_2MeCMeNH_2$)]OTf in 2 mL of H_2O was treated with 3.9 mL of 0.03 M KOH. The color of the solution changed from red to orange. After 1 min, the product was extracted into 5 mL of CH_2Cl_2. The extract was concentrated to dryness to give an orange oil whose ^1H NMR spectrum matched that of the known [(cymene)Ru(η^4-SC_3H_2-MeCOMe)] (kinetic isomer).[2]

[(cymene)Ru(η^4-C_4Me_4S-2-NH_2)]BF_4 (4). Anhydrous NH_3 was bubbled through a solution of 200 mg (0.36 mmol) of [(cymene)Ru(C_4Me_4S)]$(BF_4)_2$ in 15 mL of CH_3CN for 1 min. The color of the reaction solution changed to bright yellow. After the solvent was removed, the residue was extracted into 15 mL of CH_2Cl_2. The filtrate was filtered away from the NH_4-OTf and diluted with hexanes to give yellow crystals. Yield: 150 mg (86%). ^1H NMR (acetone-d_6): 6.09 (m, 1H), 6.0 (m, 1H), 5.82 (m, 1H), 5.64 (m, 1H), 3.62 (br s, 2H, NH_2), 2.80 (sept, 1H), 2.44 (s, 3H), 2.23 (s, 3H), 2.12 (s, 3H), 1.74 (s, 3H), 1.68 (s, 3H), 1.29 (dd, 6H). $^{13}C\{^1H\}$ NMR (acetone-d_6): 114.6 (^{i}-PrC_6H_4Me), 108.5 ($SC_4Me_4NH_2$), 102.5 ($^iPrC_6H_4Me$), 95.8 (SC_4-Me_4NH_2), 88.9 ($^iPrC_6H_4Me$) , 87.6 ($^iPrC_6H_4Me$), 86.1 ($^iPrC_6H_4$-Me), 85.4 ($^iPrC_6H_4Me$), 85.3 ($SC_4Me_4NH_2$), 77.2 ($SC_4Me_4NH_2$), 32.2 ($CH(Me)_2C_6H_4Me$), 24.0, 23.4, 23.2, 18.6, 17.2, 13.8, 13.2. IR: ν_{NH} = 3431 and 3352 cm^{-1}. FAB-MS: 392 (M^+). Anal. Calcd for $C_{18}H_{28}NBF_4RuS$: C, 45.20; H, 5.90; N, 2.90; Ru, 21.10; S, 6.70. Found: C, 45.19; H, 5.93; N, 2.91; Ru, 21.27; S, 6.64.

Reaction of 4 with HOTf. Addition of 9.0 μL (0.115 mmol) of HOTf to a solution of 50 mg (0.105 mmol) of [(cymene)Ru-(η^4-C_4Me_4S-2-NH_2)]BF_4 in 8 mL of CH_2Cl_2 precipitated a yellow solid, which was collected and recrystallized from acetone/Et_2O. ^1H NMR spectroscopy showed that the product was [(cymene)Ru(C_4Me_4S)]$^{2+}$.[9]

[(C_5Me_5)Rh(η^4-C_4Me_4S-2-NH_2)]OTf (5). A pale yellow solution of 200 mg (0.295 mmol) of [(C_5Me_5)Rh(C_4Me_4S)]$(OTf)_2$ in 15 mL of CH_3CN was purged with gaseous NH_3 for ~1 min, resulting in a yellow-orange solution. The solvent was removed, and the residue was extracted into 15 mL of CH_2Cl_2, leaving a white residue of NH_4OTf. The solution was concentrated to 2 mL and diluted with 15 mL of hexanes, affording light orange microcrystals. Yield: 140 mg (87%). ^1H NMR (CD_3CN): 3.10 (br s, 2H, NH_2), 2.28 (s, 3H), 1.92 (d, J_{H-Rh} = 1.0, 3H), 1.83 (s, 15H, C_5Me_5), 1.69 (s, 3H), 1.48 (s, 3H), ^{13}C-$\{^1H\}$ NMR (acetone-d_6): 122.1 (q, CF_3), 108.8 (d, J = 2.28), 99.9 (d, J = 6.87, C_5Me_5), 99.1 (d, J = 6.87), 91.5 (d, J = 9.15),

Table 1. Selected Bond Distances (Å) and Angles (deg) of $[(C_6Me_6)Ru(\eta^4\text{-}SC_3H_2MeCHNHPh)]PF_6$ (7) and $[(\text{cymene})Ru(\eta^4\text{-}SC_3H_2MeCMeNHPh)]OTf$ ($\mathbf{8}_{\text{therm}}$)

	7	8_{therm}
Ru–S	2.335(3)	2.392(6)
Ru–C2	2.192(5)	2.160(2)
Ru–C3	2.222(10)	2.14(2)
Ru–C4	2.288(6)	2.22(2)
Ru–C5	2.627(6)	3.08(2)
S–C2	1.74(3)	1.73(2)
C2–C3	1.39(3)	1.36(2)
C3–C4	1.435(11)	1.44(2)
C4–C5	1.389(10)	1.46(2)
C5–N	1.348(8)	1.34(2)
N–C6	1.433(9)	1.47(2)
Ru–C_{6R6}	2.218(3)–2.222(3)	2.17–2.29(2)
S–C2–C3	120.7(5)	121(1)
C2–C3–C4	127.8(10)	115(2)
C3–C4–C5	129.0(7)	122(2)
C4–C5–N	120.4(6)	123(2)
C5–N–C6	124.8(6)	124(1)
C2–C3–C4	127.8(10)	115(2)
C3–C4–C5	129.0(7)	122(2)
C4–C5–N	120.4(6)	123(2)
C5–N–C6	124.8(6)	124(1)

81.9 (d, J = 10.68), 24.4, 15.0, 11.1, 10.7, 9.3 (C_5Me_5). IR: ν_{NH} = 3407 and 3330 cm^{-1}. FAB-MS: 394 (M$^+$). Anal. Calcd for $C_{19}H_{29}NF_3O_3RhS_2$: C, 41.99; H, 5.38; N, 2.58; Rh, 18.94; S, 11.8. Found: C, 41.87; H, 5.37; N, 2.52; Rh, 18.58; S, 12.0.

Reaction of $[(C_5Me_5)Rh(\eta^4\text{-}C_4Me_4S\text{-}2\text{-}NH_2)]OTf$ with HOTs. Addition of 30 mg (0.178 mmol) of $HOSO_2C_6H_4Me{\cdot}H_2O$ to a solution of 70 mg (0.13 mmol) of $[(C_5Me_5)Rh(\eta^4\text{-}C_4Me_4S\text{-}2\text{-}NH_2)]OTf$ in 10 mL of CH_2Cl_2 precipitated a yellow solid, which was collected and recrystallized from acetone/Et_2O. The product was identified as $[(C_5Me_5)Rh(C_4Me_4S)]^{2+}$ by its ^1H NMR spectrum.[1]

$[(C_6Me_6)Ru(\eta^4\text{-}SC_3H_3CHNHPh)]OTf$ (6). A solution of 200 mg of $[(C_6Me_6)Ru(C_4H_4S)](OTf)_2$ (0.31 mmol) in 20 mL of CH_3CN was treated with 56 μL (0.62 mmol) of $PhNH_2$, resulting in a color change from pale yellow to orange-red. After 3 h, the solvent was removed under vacuum and the residue was extracted into 20 mL of CH_2Cl_2, leaving a gray powder of $PhNH_3(OTf)$. The filtrate was concentrated to 2 mL and diluted with 15 mL of hexanes giving red crystals. Yield: 156 mg (85%). ^1H NMR (CD_3CN) (see eq 6 for labeling scheme): 8.02 (br d, J_{NH-H} = 12.7, 1H, N*H*Ph), 7.39 (m, 2H, C_6H_5NH), 7.10 (m, 1H, C_6H_5NH), 6.92 (m, 2H, C_6H_5NH), 6.77 (dd, $J_{1,2}$ = 11.1, 1H, H_a of SC_3H_3CHNHPh), 6.25 (d, $J_{4,3}$ = 5.4, 1H, H_d of SC_3H_3CHNHPh), 5.82 (dd, $J_{3,2}$ = 6.4, 1H, H_c of SC_3H_3CHNHPh), 4.69 (dd, 1H, H_b of SC_3H_3CHNHPh), 2.16 (s, 18H, C_6Me_6). $^{13}C\{^1H\}$ NMR (CD_3NO_2): 141.9 (C_a of SC_3H_3*C*HNHPh), 131.3 (C_6H_5NH), 126.8 (C_6H_5NH), 124.3 (C_6H_5NH), 120.4 (q, CF_3), 116.7 (C_6H_5NH), 104.1 (C_d of SC_3H_3CHNHPh), 103.0 (C_6Me_6), 90.8 (C_c of SC_3H_3CHNHPh), 75.2 (C_d of SC_3H_3CHNHPh), 16.9 (C_6Me_6). IR: ν_{NH} = 3252 cm^{-1}. FAB-MS: 440 (M$^+$) Anal. Calcd for $C_{23}H_{28}NF_3O_3RuS_2$: C, 46.92; H, 4.79; N, 2.38; Ru, 17.17; S, 10.89. Found: C, 46.93; H, 4.79; N, 2.40; Ru, 17.30; S, 10.72.

$[(C_6Me_6)Ru(\eta^4\text{-}SC_3H_2MeCHNHPh)]PF_6$ (7). A solution of 200 mg (0.307 mmol) of $[(C_6Me_6)Ru(2\text{-}MeC_4H_3S)](PF_6)_2$ in 10 mL of CH_3CN was treated with 56 μL (0.614 mmol) of $PhNH_2$, resulting in a color change from pale yellow to purple-red. After 10 min, the solvent was removed under vacuum and the residue was extracted into 8 mL of CH_2Cl_2, leaving a gray powder of $PhNH_3(PF_6)$. The filtrate was concentrated to 2 mL and diluted with 15 mL of hexanes, giving a red powder. A CH_2Cl_2 solution of this product was further purified by chromatography on silica gel. Yield: 137 mg (75%). ^1H NMR (CD_3CN) (see eq 6 for labeling scheme): 9.02 (br d, J_{NH-H} = 12.7, 1H, N*H*Ph), 7.42 (m, 2H, C_6H_5NH), 7.11 (m, 1H, C_6H_5NH), 6.99 (m, 2H, C_6H_5NH), 6.97 (dd, 1H, H_a of SC_3H_2MeC*H*NHPh), 5.87 (d, $J_{3,2}$ = 6.6, 1H, H_c of SC_3H_2MeCHNHPh),

Table 2. Atomic Coordinates and Equivalent Isotropic Thermal Parameters for 7

	x	y	z	U(eq), Å^2
Ru	−361(1)	2500	1441(1)	23(1)
S	1508(3)	3903(2)	870(1)	26(1)
N	3440(7)	1350(5)	2721(3)	31(1)
C1	−46(8)	2687(14)	−501(3)	32(3)
C2	858(7)	2569(34)	328(3)	26(2)
C3	1186(14)	1380(10)	648(6)	29(2)
C4	1900(8)	1067(6)	1438(4)	28(1)
C5	2877(8)	1816(7)	2002(4)	28(1)
C6	4302(16)	2067(8)	3363(5)	29(2)
C7	5059(17)	1428(8)	4024(5)	36(2)
C8	5870(16)	2084(7)	4666(5)	33(3)
C9	5862(17)	3379(8)	4657(5)	39(2)
C10	5108(18)	4001(8)	3996(6)	35(2)
C11	4302(17)	3352(8)	3354(6)	35(2)
C12	−1475(6)	2500	2610(3)	38(1)
C13	−1911(4)	3652(3)	2213(2)	36(1)
C14	−2828(4)	3645(3)	1437(2)	35(1)
C15	−3269(6)	2500	1052(3)	34(1)
C18	−548(3)	2500	3432(3)	67(2)
C19	−1431(7)	4892(4)	2615(3)	70(1)
C20	−3341(6)	4868(4)	1023(3)	63(1)
C21	−4214(7)	2500	222(3)	61(2)
P1	3343(3)	7536(16)	2560(1)	45(1)
F1	3048(13)	8747(7)	2028(5)	98(3)
F2	3659(16)	6379(8)	3100(5)	118(3)
F3	1335(7)	7234(11)	2348(3)	102(3)
F4	5328(8)	7914(8)	2738(5)	134(4)
F5	3709(12)	6758(8)	1818(5)	101(3)
F6	2816(13)	8347(9)	3289(5)	99(3)
Cl	1169(3)	3848(2)	5365(1)	101(1)
C24	1376(21)	2500	5917(5)	136(5)

4.82 (dd, $J_{2,1}$ = 10.9, 1H, H_b of SC_3H_2MeCHNHPh), 2.30 (s, 3H, Me_d of SC_3H_2*Me*CHNHPh), 2.21 (s, 18H, C_6Me_6). $^{13}C\{^1H\}$ NMR (acetone-d_6): 141.3, 141.2, 130.6, 123.6, 115.9, 115.8, 101.3, 87.5 (C_c of SC_3H_2MeCHNHPh), 73.0 (C_b of SC_3H_2MeCHNHPh), 28.65 (Me_d of SC_3H_2*Me*CHNHPh), 16.15 (C_6Me_6). IR: ν_{NH} = 3364 cm^{-1}. FAB-MS: 454 (M$^+$). Anal. Calcd for $C_{23}H_{30}NF_6O_3PRuS{\cdot}0.3CH_2Cl_2$: C, 44.84; H, 4.94; N, 2.24. Found: C, 44.96; H, 4.95; N, 2.35.

$[(\text{cymene})Ru(\eta^4\text{-}SC_3H_2MeCMeNHPh)]OTf$ (8). A solution of 200 mg (0.31 mmol) of $[(\text{cymene})Ru(2,5\text{-}Me_2C_4H_2S)](OTf)_2$ in 10 mL of CH_3CN was treated with 60 μL (0.62 mmol) of $PhNH_2$, resulting in a color change from pale yellow to purple-red. After 10 min, the solvent was removed under vacuum and the residue was extracted into 8 mL of CH_2Cl_2 to give a red solution and gray powder of $PhNH_3(OTf)$. The CH_2Cl_2 extract was filtered, concentrated to 2 mL, and diluted with 15 mL of hexanes, giving 160 mg (88%) of purple-red needle crystals. The ^1H NMR spectrum showed two thermodynamic isomers formed in a ratio of 4:1. ^1H NMR (CD_3CN, major isomer of $\mathbf{8}_{\text{therm}}$) (see eq 7 for labeling scheme): 10.51 (br s, 1H, N*H*), 7.51 (m, 2H), 7.39 (m, 3H), 5.96 (d, J = 6.8, 1H, H_c of SC_3H_2MeCMeNHPh), 5.76 (m, 1H), 5.68 (ps d, 1H), 5.63 (ps d, 1H), 5.11 (ps d, 1H), 2.39 (s, 3H), 2.37 (s, 3H), 2.18 (s, 3H), 1.93 (sept, 1H), 1.86 (d, J = 7.0, 1H, H_b of SC_3H_2MeCMeNHPh), 1.26 (dd, 6H). $^{13}C\{^1H\}$ NMR (acetone-d_6, major isomer): 185.0 (C_a of SC_3H_2Me*C*MeNHPh), 137.1, 130.2, 129.0, 125.0, 122.1 (q, CF_3), 111.3, 109.8, 100.1, 86.6, 85.3, 85.1, 84.9, 84.2, 83.7, 55.7 (C_b of SC_3H_2MeCMeNHPh), 32.3, 26.8, 23.8, 23.6, 21.2, 18.6. IR: ν_{NH} = 3223 cm^{-1}. FAB-MS: 440 (M$^+$). Anal. Calcd for $C_{23}H_{28}NF_3O_3RuS_2$: C, 46.92; H, 4.79; N, 2.38; Ru, 17.17; S, 10.89. Found: C, 46.88; H, 4.84; N, 2.38; Ru, 17.08; S, 10.93. In an NMR tube, a solution of 30 mg (0.047 mmol) of $[(\text{cymene})Ru(2,5\text{-}Me_2C_4H_2S)](OTf)_2$ in 0.65 mL of CD_3CN was cooled to −10 °C and treated with 10 μL (0.10 mmol) of $PhNH_2$, resulting in a color change from pale yellow to purple-red. The reaction was monitored by ^1H NMR spectroscopy at −10 °C, which showed that only one kinetic isomer formed, isomerizing to two thermodynamic isomers upon warming to ambient temperatures. ^1H NMR (CD_3CN, −10 °C, $\mathbf{8}_{\text{kin}}$): 8.02 (br s, 1H, N*H*), 7.35 (m, 3H), 7.10 (m, 2H), 6.01 (ps d, 1H), 5.76 (ps d,

Table 3. Atomic Coordinates for 8_{therm}

	x/a	*y/b*	*z/c*
Ru	0.1486(1)	0.09637(5)	0.0
S	0.1211(5)	0.0704(2)	0.3042(8)
N	0.074(1)	0.2358(5)	0.061(2)
C1	0.351(1)	0.0576(6)	0.269(2)
C2	0.252(1)	0.0904(6)	0.238(2)
C3	0.266(1)	0.1343(6)	0.164(2)
C4	0.166(1)	0.1627(6)	0.159(2)
C5	0.159(2)	0.2048(6)	0.052(2)
C6	−0.022(1)	0.2309(6)	0.186(2)
C7	0.247(2)	0.2193(6)	−0.076(2)
C8	−0.044(2)	0.2663(6)	0.299(2)
C9	−0.136(2)	0.2648(7)	0.404(2)
C10	−0.211(2)	0.2276(7)	0.411(2)
C11	−0.185(2)	0.1913(6)	0.288(2)
C12	−0.091(1)	0.1915(6)	0.184(2)
C13	0.181(1)	0.0299(7)	−0.168(3)
C14	0.239(2)	0.0707(6)	−0.240(2)
C15	0.178(1)	0.1139(6)	−0.288(2)
C16	0.059(1)	0.1184(6)	−0.260(2)
C17	0.003(2)	0.0808(6)	−0.177(2)
C18	0.065(2)	0.0385(7)	−0.138(3)
C19	0.239(2)	−0.0163(7)	−0.130(2)
C20	0.192(3)	−0.048(1)	−0.278(4)
C21	0.366(2)	−0.011(1)	−0.148(5)
C22	−0.005(2)	0.1624(7)	−0.310(3)
S2A	0.4544(6)	−0.1554(3)	−0.7896(10)
O1A	0.5693(7)	−0.1418(5)	−0.774(2)
O2A	0.430(1)	−0.2026(3)	−0.729(2)
O3A	0.4020(10)	−0.1423(4)	−0.956(1)
C23A	0.3826(9)	−0.1173(4)	−0.620(1)
F1A	0.401(2)	−0.0740(3)	−0.664(2)
F2A	0.2778(8)	−0.1272(7)	−0.626(2)
F3A	0.425(1)	−0.1273(5)	−0.465(1)
S2B	0.462(1)	−0.1602(5)	−0.735(2)
O1B	0.409(2)	−0.2019(6)	−0.806(3)
O2B	0.548(1)	−0.141(1)	−0.848(3)
O3B	0.489(2)	−0.1625(8)	−0.547(2)
C23B	0.349(2)	−0.1147(7)	−0.744(2)
F1B	0.314(2)	−0.1128(10)	−0.908(3)
F2B	0.392(3)	−0.0751(6)	−0.694(4)
F3B	0.271(2)	−0.128(1)	−0.636(4)

1H), 5.73 (ps d, 1 H), 5.61 (ps d, 1H), 5.43 (d, J = 5.1, 1H, H_c of SC_3H_2MeCMeNHPh), 4.10 (d, J = 5.1, 1H, H_b of SC_3H_2-MeCMeNHPh), 2.69 (sept, 1H), 2.28 (s, 3H), 2.18 (s, 3H), 2.05 (s, 3H), 1.24 (dd, 6H).

Reaction of 8_{therm} with NH_3. Gaseous NH_3 was passed over a solution of 50 mg (0.085 mmol) of **8** in 10 mL of CH_3CN for 30 s. The color of the solution changed to purple-red. The solution was evaporated to dryness. The residue was dissolved in acetone-d_6 and examined by ^1H NMR spectroscopy which established that the mixture consisted of $PhNH_2$ and the thermodynamic isomer of $[(cymene)Ru(\eta^4\text{-}SC_3H_2MeCMeNH_2)]^+$.

Crystallographic Characterization of 7. Red, prismatic crystals of $[(C_6Me_6)Ru(\eta^4\text{-}SC_3H_2MeCHNHPh)]PF_6{\cdot}CH_2Cl_2$ were obtained by layering a CH_2Cl_2 solution with diethyl ether. The crystal of dimensions 0.40 × 0.32 × 0.22 mm was mounted in oil (Paratone-N, Exxon) to a thin glass fiber with the (212) scattering planes roughly normal to the spindle axis. The salt crystallized in the monoclinic space group $P2_1/m$, with a = 7.528(2) Å, b = 10.665(2) Å, c = 17.029(4) Å, $\alpha = \gamma = 90°$, β = 96°, Z = 2, and d_{calcd} = 1.669 g/cm^3. The data crystal was bound by the (001), (00$\bar{1}$), (011), (0$\bar{1}\bar{1}$), (10$\bar{1}$), and ($\bar{1}$01) faces. Distances from the crystal center to these facial boundaries were 0.11, 0.11, 0.16, 0.16, 0.20, and 0.20 mm, respectively. Data were measured at 198 K on an Enraf–Nonius diffractometer. Systematic conditions suggested the ambiguous space group $P2_1$; however, refinement supported the presence of a symmetry center. Periodically monitored standard intensities showed no decay. Step-scanned intensity data were reduced by profile analysis[15] and corrected for Lorentz–polarization effects and for absorption.[16] Scattering factors and anomalous dispersion terms were taken from standard tables.[17]

Table 4. Crystal Data and Structure Refinement for 7

empirical formula	$C_{24}H_{32}Cl_2F_6NPRuS$
formula weight	683.51
temperature	198(2) K
wavelength	0.710 73 Å
crystal system	monoclinic
space group	$P2_1/m$
unit cell dimensions	a = 7.528(2) Å, b = 10.665(2) Å, c = 17.029(4) Å, $\alpha = \gamma = 90°$, β = 96.00(2)°
volume	1359.75(5) Å^3
Z	2
density (calculated)	1.669 Mg/m^3
absorption coefficient	0.956 mm^{-1}
F(000)	692
crystal size	0.40 × 0.32 × 0.22 mm
θ range for data collection	2.26 to 24.95°
index ranges	$0 \le h \le 8$, $0 \le k \le 12$, $-20 \le l \le 20$
reflections collected	2723
no. of independent reflections	2519 [R(i) = 0.0217]
absorption correction	integration
max and min transmission	0.8411 and 0.7135
refinement method	full-matrix least-squares on F^2
data/restraints/parameters	2519/145/280
goodness-of-fit on F^2	1.135
final R indices [$I > 2\sigma(I)$]	R_1 = 0.0357, R_{w2} = 0.0894
R indices (all data)	R_1 = 0.0400, R_{w2} = 0.0918
extinction coefficient	0.0022(6)
largest diff peak and hole	0.546 and −0.755 e/Å^3

The structure was solved in the acentric space group $P2_1$ by Patterson methods (Sheldrick, 1990); positions Ru and P1 were deduced from a vector map. Partial structure expansion revealed positions for the remaining non-H atoms including disordered positions with pseudomirror symmetry for both the anion and the asymmetric ligand of the cation. Subsequent calculations imposed mirror symmetry on the cation, anion, and solvate molecules in the centric space group $P2_1/m$. Methyl H atom positions $C{-}CH_3$, were optimized by rotation about C−C bonds while maintaining idealized C−H, C− −H, and H− −H distances were maintained. Positions for atoms H3−H6 were independently refined. Remaining H atoms were included as fixed idealized contributors. H atom U's were assigned as 1.2 U_{eq} of adjacent non−H atoms. Geometric restraints were imposed on both disordered moieties. Octahedral geometry with an effective standard deviation of 0.03 Å was imposed on the anion; the mean P−F bond length converged at 1.562(6) Å. Phenyl carbon atoms C6−C11 were restrained to have equivalent 1,2- and 1,3-distances (esd = 0.02 Å). No restraints were imposed on atomic positions S, C2−C5, N6, or H3−H5. Rigid bond restraints were imposed on the anisotropic displacement parameters refined for all non-H atoms. Successful convergence of the full-matrix least-squares refinements on F^2 was indicated by the maximum shift/error for the last cycle.[18] The highest peak in the final difference Fourier map was in the vicinity of solvate molecule; the final map had no other significant features. A final analysis of variance between observed and calculated structure factors showed no dependence on amplitude or resolution. Selected bond distances and angles are presented in Table 1, refined atomic coordinates are presented in Table 2, and crystal data and structure refinement parameters are presented in Table 4.

(15) Coppens, P.; Blessing, R. H.; Becker, P. *J. Appl. Crystallogr.* **1972**, *7*, 488.

(16) Sheldrick, G. M. *SHELX-76*: *Program for Crystal Structure Determination*; University of Cambridge: Cambridge, England.

(17) Wilson, A. J. C., Ed. *International Tables for X-ray Crystallography*; Kluwer Academic Publishers: Dordrecht, The Netherlands, Vol. C.

(18) Sheldrick, G. M. *SHELX-93*: *A Program for Structure Refinement*; University of Göttingen: Göttingen, Germany, 1994.

Table 5. Crystal Data and Structure Refinement for 8_{therm}

empirical formula	$C_{23}H_{28}F_3NO_3PRuS_2$
formula weight	588.67
crystal system	orthorhombic
wavelength	0.710 73 Å
temperature	−75 °C
space group	$Pna2_1$
unit cell dimensions	a = 11.935(3) Å, b = 28.162 (11) Å, c = 7.407 (2) Å, $\alpha = \beta = \gamma = 90°$
volume	2490 Å^3
Z	4
density (calculated)	1.570 g/cm^3
absorption coefficient	μ = 8.24 cm^{-1}
F(000)	1200
crystal size	0.07 × 0.08 × 0.05 mm
radiation	Mo $K\alpha$
scan mode	$\omega-2\theta$
scan limits	$2° < 2\theta < 51°$
scan rate	2−8°/min
no. of data collected	3029
no. of data observed	1286
no. of variables	182
R^a	0.062
$R_w{}^b$	0.049
maximum shift/error	0.05
weighting scheme	1.40
highest peak in final diff map	+0.75 > e/Å > −0.78
refinement method	SHELXS-86

^{a} $R = \Sigma(|F_o| - |F_c|)/\Sigma|F_o|$. ^{b} $R_w = [(\Sigma w(|F_o| - |F_c|)^2/\Sigma w|F_o|^2]^{1/2}$.

Crystallographic Characterization of 8_{therm}. The purple-red, translucent, and columnar crystals of [(cymene)Ru(η^4-SC_3H_2MeCMeNHPh)]OTf were obtained by layering a CH_2Cl_2 solution with hexanes. The crystal of dimensions 0.07 × 0.08 × 0.50 mm was mounted in oil (Paratone-N) to a thin glass fiber and then cooled to −75 °C with the ($\bar{1}1\bar{8}$) scattering planes roughly normal to the spindle axis. The salt crystallized in the orthorhombic space group $Pna2_1$ with a = 11.935(3) Å, b = 28.162(11) Å, c = 7.407(22) Å, $\alpha = \beta = \gamma = 90°$, Z = 4 and d_{calcd} = 1.570 g/cm^3. The structure was solved by Patterson methods;[19] the correct Ru atom position was deduced from a vector map, and partial structure expansion revealed positions for the S atom. Subsequent least-squares refinement and difference Fourier syntheses gave positions for the remaining non-H atoms, including disordered positions for all anion atoms in addition to cation C20 and C21. Equivalent 3-fold symmetry was imposed on the disordered anion positions and a common C−C bond length was imposed on the disordered methyl atoms C20 and C21. No N-bound H atom position ever surfaced. Disordered H atoms positions were not included in structure factor calculations; however, the remaining H atoms were included as fixed contributors in "ideal" positions. Common isotropic thermal parameters were refined for the H atoms, the disordered methyl C atoms of the cation, and the S, F, O, and C atoms of the anion. Anisotropic thermal coefficients were refined for the Ru, N, and cation S atoms, and independent isotropic thermal coefficients were refined for the ordered C atoms. Successful convergence was indicated by the maximum shift/error for the last cycle. The highest peak in the final difference Fourier map was in the vicinity of the anion. A final analysis of variance between observed and calculated structure factors showed dependence on sin θ and amplitude. Selected bond distances and angles are presented in Table 1, refined atomic coordinates are presented in Table 3, and crystal data and structure refinement parameters are presented in Table 5.[20]

Acknowledgment. This research was supported by the U.S. Department of Energy. We thank H. Krautscheid, A. K. Verma, and T. Prussak for assistance.

Supplementary Material Available: Labeled ORTEP diagrams and tables of bond distances, bond angles, and thermal parameters (11 pages). Ordering information is given on any current masthead page.

OM950104W

(19) Sheldrick, G. M. *Acta Crystallogr.* **1990**, *A46*, 467.

(20) Plots in Figures 1 and 2 employed A. L. Spek's PLATON-92 software (Vakgroep Kristalen Structuurchemie, University of Utrecht, Padualaan 8, 3584 CH Utrecht, The Netherlands, 1992).